

Fatigue Life Prediction for Solder Interconnects in IGBT Modules for Hybrid Vehicle Application



#¹Dipesh Kumbhakarna, #²Farook Sayyad

¹kddipesh.1991@gmail.com

²fbsayyad@gmail.com

#²G.S.M.C.O.E, Balewadi, Pune, India

ABSTRACT

Insulated gate bipolar transistors are the power semiconductors used for high current applications as a switching device. It is widely used in electrical and hybrid vehicles. It has become increasingly important to understand the reliability of these modules. The lifetime prediction is based on the assumption that the solder interconnections are the weakest part of the module assembly and that the failure cause is the inelastic deformation energy accumulated within the solder material. In this paper, the effects of thermo-mechanical fatigue of the solder layer interface have been investigated. A 2D model of 6 pack, 1200V IGBT module is used for the analysis. This study presents simulation of crack initiation and propagation under thermo-mechanical loading. Successive initiation technique is used to propagate crack in solder layer. A cyclic creep-fatigue damage under thermal loading is modeled using Energy Partitioning model to predict the fatigue life of an IGBT module.

Keywords— Successive initiation technique, IGBT, Energy partitioning model, Finite element analysis.

ARTICLE INFO

Article History

Received : 18th November 2015

Received in revised form :
19th November 2015

Accepted : 21st November ,
2015

Published online :
22nd November 2015

I. INTRODUCTION

Now a day's many companies are working on hybrid vehicle and electrical vehicle. Main Inverter, DC/DC Converter, Auxiliary Inverters/Converters, Battery Management and On-board Charger are the components of HEV and EV. Figure 1 shows all the components.

Main Inverter: With an electric drivetrain, the inverter controls the electric motor. This is a key component in the car as, similar to the Engine Management System (EMS) of combustion vehicles, it determines driving behavior. Not only does the inverter drive the electric motor, it also captures energy released through regenerative braking and feeds this back to the battery. As a result, the range of the vehicle is directly related to the efficiency of the main inverter.

DC/DC Converter: Different voltage levels are required by the various electronic components in an EV. High-voltage batteries with different voltage levels are currently available on the market. In addition, the power classes scale from 1kW to 5kW depending on the number of low-voltage applications. In EVs and HEVs, the DC/DC

converter supplies the 12V power system from the high voltage battery.

Auxiliary Inverters/Converters: Power on demand increases the efficiency of electric vehicles. With HEVs and EVs, former belt-driven devices classified as auxiliary drives have been electrified and integrated into the power system to deliver power on demand. Typical auxiliary systems supplied from the high-voltage battery include air conditioning, electronic power excellent thermo-mechanical stability with effective thermal management of IGBT chips. **Battery Management:** The battery management system controls battery state during charging and discharging. Intelligent functionality is needed to extend the battery lifetime, which has a considerable impact on the total cost of ownership. The State of Health (SoH), State of Charge (SoC) and Depth of Discharge (DoD) of the battery is permanently monitored.

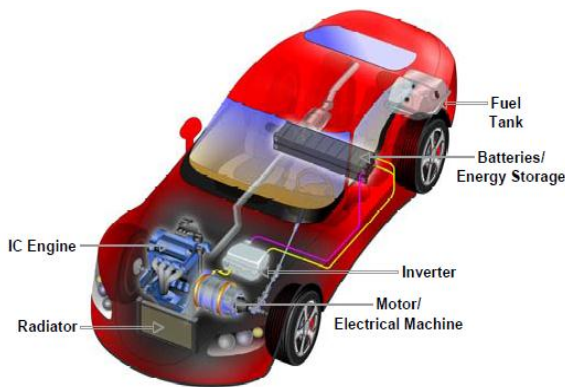


Figure 1. Shows components of HEV

On-board Charger: The battery in an electric vehicle is useless without a battery charger. And all electronic systems depend on the battery for power. With an on-board charger unit, the battery can be charged from a standard power outlet. This is a very important function of electrical vehicle.

Power modules contain one or more semiconductor switches packaged together for easy connectivity. Power semiconductor modules play a key role in power electronic systems. The module can be used to enclose thyristors, diodes, FET, IGBT, or similar semiconductor switches. Nowadays, IGBTs are widely used as a result of good switching performance combined with fairly low conduction losses [1]. IGBT is a four layer semiconductor device. It combines the voltage characteristics of a bipolar transistor and the drive characteristics of a MOSFET. The popularity of the IGBT has increased in recent years due to an increase in high voltage, high power applications. They are available in the range of voltage rating from 300 to 1200 volts and current rating from 15 to 100 amps for a single die. IGBT modules have current ratings well into the 100's of amps [2].

IGBT power modules are used in applications like automotive, traction, solar inverters. In hybrid electric vehicles, an electric power conversion system that includes an inverter and converter. They are used to convert the power generated by the engine into electrical energy, to charge and discharge a battery, and to drive the motor. The electric power conversion system typically uses an IGBT module as its main switching device. The failure modes that have been identified are Al wire bond failure and crack in the solder layer between the base plate and substrate. Hence, the major concern from the reliability standpoint of view is the effect of thermal cycling on the insulating substrate to the base-plate solder interface. In this study, fatigue life prediction for solder interconnects in IGBT module by using E-P damage model and the SI method is done.

Prof. Abhijit Dasgupta's group at University of Maryland has developed the successive initiation method and the examples of the use of the SI method are listed in this section. Dr. Juscelino Okura introduced SI method which can be used with any damage model [3]. Ladani et al. have discussed the use of SI method for lead-free BGA solder interconnects [3]. In this research an experiment was designed

and implemented on printing and reflow processes of Pb-free solder interconnects in order to obtain error-seeded specimens. The specimens were characterized for voids and subjected to temperature cycling in order to evaluate the durability of specimens under thermo-mechanical loading. Statistical analysis of the void characterization as well as durability suggested the detrimental effect of voids. To verify this observation and in order to quantify the detailed influence of size, location, and volume fraction of voids, extensive modeling was conducted. A global-local modeling approach was used to model an error seeded solder ball with voids of different sizes and in different locations. An existing E-P model was modified by SI method and used to explicitly predict damage initiation and propagation in BGA solder joints. Two techniques were used to predict the life, averaging technique and successive initiation [3]. James Gyllenskoghas reported the use of E-P model coupled with a SI technique to see the initiation of crack and fatigue life prediction of the T-38 aileron lever for materials aluminum 2014-T6 and 7050-T74 [4].

II. BACKGROUND

Transistor is a three lead semiconductor device that acts as an electrically controlled switch or a current amplifier. BJT is a current controlled device, whereas FET and MOSFET are voltage controlled devices. The simple addition of an extra P-N junction to the drain of the MOSFET changes the unipolar device into bipolar junction transistor. Combination of an insulated gate input and bipolar output makes the IGBT an excellent power switch for medium frequency and high voltage applications. It combines features of both of these devices. Power electronics packaging technology has been developed for several generations, involving material upgrading, structure improvement and interconnection technique innovation. IGBT is presently one of the most popular devices due to its wide ratings and switching speed of about 100 KHz, which makes it an easy voltage drive. Among the new power devices, IGBT devices are being more accepted and increasingly used in traction applications such as locomotive, elevator, tram and subway.

Power semiconductor modules play a key role in power electronic systems. The module can be used to enclose thyristors, diodes, FET, IGBT, or similar semiconductor switches. The reliability of solder interconnects has always been an area of concern for microelectronics applications and continues to be a concern for power electronics as well. The study has been done by Hua Ye et al [5], on different failure modes in power electronic devices. They concluded that thermal cycling has a significant effect on the solder layer reliability. They also stated that using finite element analysis and damage mechanics constitutive model it is possible to predict the number of cycles to failure for solder layers. Sun et al [6] proposed CZM-based thermo-mechanical fatigue model. This model was developed to simulate the delamination process at the die-solder interface and to predict the lifetime of solder joint in IGBT module. In this model the path of the crack is known. To analyze this crack propagation process by delamination, a very thin layer of the solder joint at the die-solder interface is replaced by a

layer of cohesive elements with the same thickness. The damage will be concentrated on this cohesive layer which allows simulating the progressive crack initiation and propagation taking place at the die-solder interface. The thickness of the cohesive layer will influence more or less the thermo-mechanically induced strain and stress fields. Hence, the effect of the thickness on the rate of damage evolution and the lifetime is studied. There are several different approaches like stress based approach, strain based approach, energy based approach and E-P damage model approach that are used to predict the life of solder joints. Present study focuses on fatigue life prediction for solder interconnects in IGBT module by using SI technique and E-P model. SI technique is used to propagate crack in solder layer interface between substrate and base plate. E-P damage model approach is used to predict the lifetime of an IGBT module. E-P damage model assumes that cyclic fatigue damage is due to combination of elastic, plastic and creep deformation mechanism[3].

III. MODELING METHODOLOGY

A 2D IGBT module is used for the analysis. Module contains die soldered onto a DBC substrate which is made out of Aluminum Nitride (AlN) material for internal electrical insulation. It is then soldered to the base plate. Figure 1 shows a 2D view of the multi-layer IGBT structure.

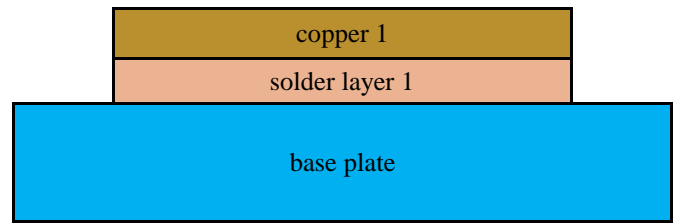


Figure 1: Schematic diagram of a conventional IGBT module[7].

Table 1. Dimensions of IGBT module

Part	Material	Total Dimensions (mm)
Die	Silicon	12.7 x 12.7 x 0.42
Solder Layer 2	SAC305	12.7 x 12.7 x 0.08
Copper 2	Copper	41.7 x 27.5 x 0.3
Substrate	AlN	41.7 x 27.5 x 0.6
Copper 1	Copper	41.7 x 27.5 x 0.3
Solder Layer 1	SAC305	41.7 x 27.5 x 0.21
Base Plate	AlSiC	174.1 x 92 x 3

Table 2. Material properties used for IGBT module

Mesh sensitivity analysis was carried out where plastic work varies in the range of +/-2%. Figure 2 shows 2D finite element model of IGBT module. Element plane 183 is used for the analysis.

Part	Material	Young Modulus (Gpa)	Poisson's ratio	CTE (ppm/°c)
Die	Silicon	131	0.3	2.8
Solder Layer 2	SAC305	MISO Properties		20
Copper 2	Copper	121	0.3	17.3
Substrate	AlN	330	0.24	4.5
Copper 1	Copper	121	0.3	17.3
Solder Layer 1	SAC305	MISO Properties		20
Base Plate	AlSiC	188	0.29	8.75

Dimensions of each layer within the module construction are given in Table 1.

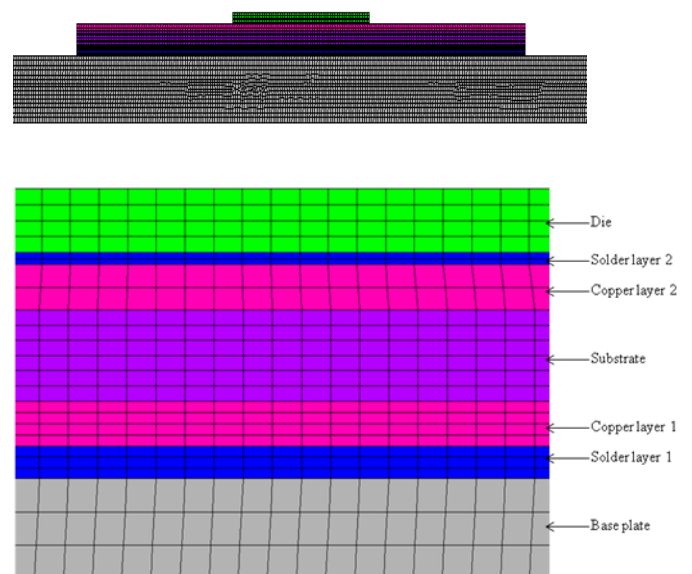
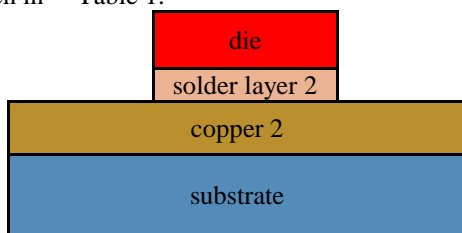


Figure 2: Two dimensional finite element meshed structure

Material properties used for the analysis are given in Table 2. The solder layer is modeled using multi-linear isotropic properties and creep properties. The primary creep is neglected due to negligible damage in thermal cycling. Secondary creep is considered for the analysis. For solder materials Garofalo constants are used which are provided in Table 3[8].

Solder alloy	Creep properties			
	α (MPa) ⁻¹	n_c	A	Q(J·mol-K)
SAC305	0.18	2.3	6.07	55793

Table 3. Secondary creep Garofalo constants[8]

IGBT module is subjected to thermal cycles ranging from -55°C to 160°C and 0°C to 100°C with 15 min ramps and 15 min dwells. Figure 3 shows the thermal cycle range from -55°C to 160°C[5]. Plain strain condition is considered for the analysis. To apply boundary condition, all nodes at bottom surface of base-plate are fixed.

Below shows thermal time history for -55°C to 160°C temperature range. The results are calculated at every thermal cycle and actual results consider are difference between last thermal and second thermal cycle. This technique gives us accurate results. Temperature cycle having time period 15 minutes ramp down and ramp up, 15 minutes dwell. Total thermal cycle required 60 minutes to complete. Same thermal cycle consider for temperature range 0°C to 100°C.

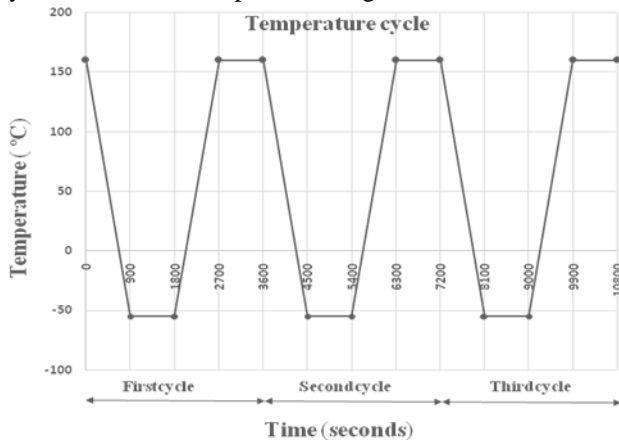


Figure 3: Thermal time history

ENERGY PARTITIONING DAMAGE MODEL

A cyclic creep-fatigue damage under thermal cycling is modeled using an E-P model. This model predicts cyclic creep fatigue damage based on deviatoric energy densities U_e , W_p and W_c for a typical load cycle. The damage due to each of these deformation mechanisms is determined by using a power law as provided in equation (1) to (3).

$$U_e = U_{e0} N_e^b \quad \dots (1)$$

$$W_p = W_{p0} N_p^c \quad \dots (2)$$

$$W_c = W_{c0} N_c^d \quad \dots (3)$$

Figure 4 shows log-log plot of elastic, plastic and creep energy density (i.e. U_e , W_p , and W_c respectively) versus cycles to failure. The exponents b, c, and d are their corresponding slopes. W_p and W_c are obtained from FEA analysis. Energy densities are calculated on those elements which are eliminated in every run.

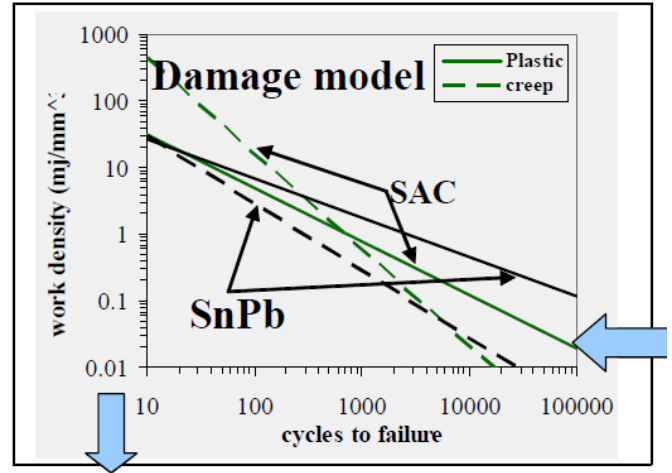


Figure 4: Work density versus number of cycles to failure [3].

Damage caused by each type of deformation can be calculated by substituting equations (1), (2) or (3) in equation (4). Damage is defined as reciprocal to number of cycles, as follows:

$$D = \frac{1}{N_f} \quad \dots(4)$$

The total damage can be calculated by adding damage caused by elastic, plastic and creep deformation as seen in equation (5). Usually damage caused by elastic deformation is negligible.

$$D_{total} = D_e + D_p + D_c \quad \dots(5)$$

$$\frac{1}{N_f} = \frac{1}{N_e} + \frac{1}{N_p} + \frac{1}{N_c} \quad \dots(6)$$

The total number of cycles to failure N_f is calculated from equation (6)[3].

SUCCESSIVE INITIATION METHOD

The SI method was first introduced by Okura[3]. SI analysis involves several steps for damage initiation and propagation shown in Figure 5. SI method is implemented with the help of finite elements. The damage initiation site is first identified with the help of an E-P damage model, for a typical cyclic loading condition. Inelastic energy includes plastic and creep work per cycle. This energy is calculated using FEA for all the elements to estimate the amount of damage by an E-P damage model. The elements with maximum damage can be identified from contour plots. The initiation zone is recognized by selecting all elements which exceed a suitable damage threshold. In order to minimize number of runs and to facilitate reasonable computational time, damage threshold in our case was selected to be 60% of the maximum value of damage. The

propagation path for maximum damage evolution is then monitored. Elements in the damage initiation zone are removed from the structure by eliminating or killing the damaged elements. The cyclic loading is repeated on the remaining surviving structure and new damage zones are identified based on 60% of the maximum value of damage. The process is incrementally repeated, until a complete failure path is established and the critical solder joint loses its ability to carry any further loads[9].

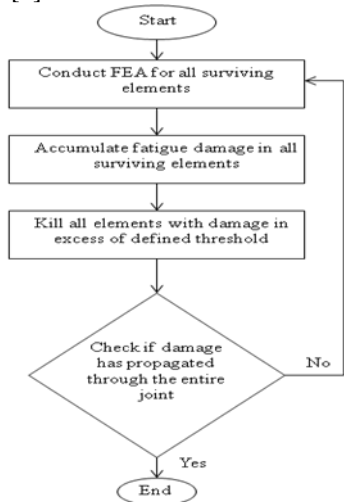


Figure 5: Damage propagation algorithm using SI method[9].

The total number of cycles to failure is calculated using MATLAB algorithm for thermal cycles ranging from -55°C to 160°C and 0°C to 100°C. Calculations and tables shown below indicate values for thermal cycle -55°C to 160°C. Similarly, values have been calculated for thermal cycle 0°C to 100°C. Following is the procedure to calculate total number of cycles to failure. The term "Run" which is used in Table 4 to Table 10, refers to the thermal cycling applied on FEA model. Calculated damage is accumulated in individual elements. The threshold damage criteria is applied to kill the elements having value excess of defined threshold. Above run procedure is repeated till the complete delamination of solder layer is achieved.

Calculated creep work values for the runs are the per cycle work (i.e. creep work developed at the end of last thermal cycles). Table 4 shows the values from run 1 to run 56. Calculated plastic work values for the runs are the per cycle work (i.e. plastic work developed in the last thermal cycle). Table 5 shows the values from run 1 to run 56. In following tables "0" value shows set of element having energy more than threshold. From values of creep work and plastic work estimate number of cycles due to creep and plastic work (N_c & N_p) by using work density versus number of cycles to failure graph (Figure 4).

Following equations are used to calculate damage due to creep and plastic work.

Table 4. Creep Work

Run 1	Run 2	Run 3	Run 4	Run 5 to Run 52	Run 53	Run 54	Run 55	Run 56
4.821	2.9004	2.259	2.0381	0.2182	0.2167	0.2158	0.2168

$$D_c = \frac{1}{N_c} \quad \dots(7)$$

$$D_p = \frac{1}{N_p} \quad \dots(8)$$

We get damage per cycle by addition of damage due to creep and plastic. Table 6 shows damage per cycle values.

$$Damage/Cycle = D_c + D_p \quad \dots(9)$$

Reciprocal of damage per cycle gives value of discrete N_f.

Table 7 shows discrete N_f values.

$$Discrete N_f = \frac{1}{Damage/Cycle} \quad \dots(10)$$

Cumulative N_f and total damage values are calculated simultaneously. First row of cumulative N_f is equal to the first row of discrete N_f. First row of total damage is equal to first column value of cumulative N_f divided by current column value of cumulative N_f.

Second row of cumulative N_f is calculated by following equation.

$$Cumulative N_f = \frac{(1 - (Total Damage)_{previous row})}{(Damage/Cycle)_{current row}} \quad \dots(11)$$

Above equation(11) is used to calculate remaining cumulative N_f values. Table 8 shows cumulative N_f values.

For e.g.

$$(Cumulative N_f)_{@Run2} = \left[\frac{(1 - 0.704992)}{0.005516} \right] = 53.4759$$

Second row of total damage is calculated by following equation.

$$Total Damage = 1 - \left[\left((Cumulative N_f)_{@Current row} - (Cumulative N_f)_{@Run 2} \right) \times (Damage per Cycle)_{@current row value} \right] \quad \dots(12)$$

Above equation(12) is used to calculate remaining total damage values. Table 9 shows total damage values.

For e.g.

$$Total Damage_{@Run3} = 1 - [(109.4635 - 53.4759) \times 0.00370] = 0.79$$

Total N_f is to addition of diagonal values of cumulative N_f[10].

Table 10 shows total N_f values.

For e.g.

$$Total N_f_{@Run 2} = 238.7731 + 53.4759 = 292.2491$$

0	7.1949	4.044	2.6716	0.2165	0.215	0.2141	0.2152
0	0	7.0335	3.9665	0.2153	0.2138	0.2129	0.2141
0	0	0	6.9603	0.2141	0.2125	0.2117	0.213
0	0	0	0
0	0	0	0
0	0	0	0	0	0.2687	0.1984	0.179	0.1742
0	0	0	0	0	0	0.2702	0.1972	0.1759
0	0	0	0	0	0	0	0.2594	0.1814
0	0	0	0	0	0	0	0	0.1978

Table 5. Plastic Work

Run 1	Run 2	Run 3	Run 4	Run 5 to Run 52	Run 53	Run 54	Run 55	Run 56
0.058659	0.065808	0.067969	0.067911	0.041073	0.040952	0.040867	0.041153
0	0.04224	0.059531	0.06837	0.040878	0.040767	0.040686	0.04099
0	0	0.042993	0.060104	0.040746	0.040643	0.040564	0.04088
0	0	0	0.043455	0.040613	0.040519	0.040443	0.040771
0	0	0	0
0	0	0	0
0	0	0	0	0	0.049481	0.041523	0.038171	0.037377
0	0	0	0	0	0	0.049407	0.04134	0.037692
0	0	0	0	0	0	0	0.047865	0.038824
0	0	0	0	0	0	0	0	0.04059

Table 6. Damage per cycle

Run 1	Run 2	Run 3	Run 4	Run 5 to Run 52	Run 53	Run 54	Run 55	Run 56
0.004188	0.002952	0.002487	0.002318	0.000500	0.000498	0.000496	0.000498
0	0.005516	0.003708	0.002792	0.000497	0.000495	0.000493	0.000495
0	0	0.005430	0.003659	0.000495	0.000493	0.000491	0.000494
0	0	0	0.005391	0.000493	0.000491	0.000490	0.000492

0	0	0	0
0	0	0	0
0	0	0	0	0	0.000581	0.000470	0.000436	0.000428
0	0	0	0	0	0	0.000583	0.000468	0.000431
0	0	0	0	0	0	0	0.000566	0.000441
0	0	0	0	0	0	0	0	0.000468

Table 7. Discrete N_f

Run 1	Run 2	Run 3	Run 4	Run 5 to Run 52	Run 53	Run 54	Run 55	Run 56
238.7731	338.6887	401.9574	431.3754	1998.0962	2007.6488	2013.4701	2006.4415
0	181.2701	269.6318	358.1388	2009.1011	2018.7513	2024.6385	2016.8406
0	0	184.1369	273.2325	2016.9404	2026.6579	2032.5948	2024.0592
0	0	0	185.4709	2024.8564	2035.2767	2040.6236	2031.3373
0	0	0	0
0	0	0	0
0	0	0	0	0	1719.8799	2127.0297	2289.5999	2334.3843
0	0	0	0	0	0	1713.7103	2136.2140	2318.1570
0	0	0	0	0	0	0	1764.3075	2267.0154
0	0	0	0	0	0	0	0	2134.4035

Table 8. Cumulative N_f

Run 1	Run 2	Run 3	Run 4	Run 5 to Run 52	Run 53	Run 54	Run 55	Run 56
238.7731	338.6887	401.9574	431.3754	1998.0962	2007.6488	2013.4701	2006.4415
0	53.4759	109.4635	159.9033	1769.0129	1778.6578	1784.5409	1776.8299
0	0	38.2350	81.1959	1722.2307	1731.9386	1737.8676	1729.5222
0	0	0	29.1619	1690.6050	1700.9063	1706.3461	1697.3686
0	0	0	0
0	0	0	0
0	0	0	0	0	22.8719	42.5959	67.0304	70.4559
0	0	0	0	0	0	15.8912	41.2002	47.2532

0	0	0	0	0	0	0	20.9027	30.6700
0	0	0	0	0	0	0	0	9.1959

Table 9.Total Damage

Run 1	Run 2	Run 3	Run 4	Run 5 to Run 52	Run 53	Run 54	Run 55	Run 56
1	0.704992	0.594025	0.553515	0.119500	0.118931	0.118587	0.119003
0	1	0.792355	0.702832	0.146117	0.145421	0.145000	0.145518
0	0	1	0.842767	0.165074	0.164287	0.163811	0.164408
0	0	0	1	0.179476	0.178615	0.178102	0.178764
0	0	0	0
0	0	0	0
0	0	0	0	0	1	0.990726	0.980713	0.979616
0	0	0	0	0	0	1	0.988152	0.986471
0	0	0	0	0	0	0	1	0.995691
0	0	0	0	0	0	0	0	1

Table 10. Total N_f

Run 1	Run 2	Run 3	Run 4	Run 5 to Run 52	Run 53	Run 54	Run 55	Run 56
238.7731	238.7731	238.7731	238.7731	238.7731	238.7731	238.7731	238.7731
0	292.2491	292.2491	292.2491	292.2491	292.2491	292.2491	292.2491
0	0	330.4841	330.4841	330.4841	330.4841	330.4841	330.4841
0	0	0	359.6461	359.6461	359.6461	359.6461	359.6461
0	0	0	0
0	0	0	0
0	0	0	0	0	2220.511	2220.511	2220.511	2220.511
0	0	0	0	0	0	2236.403	2236.403	2236.403
0	0	0	0	0	0	0	2257.305	2257.305
0	0	0	0	0	0	0	0	2266.5017

IV. RESULTS

The fatigue lifetime is often represented by the number of cycles to failure. Fatigue damage in solder layer was found due to accelerated thermal cycle. The number of cycles to failure of the IGBT module are around 2266 cycles and 2400 cycles for thermal cycles -55°C to 160°C and 0°C to 100°C respectively. Figure 6 shows the 2D IGBT module before crack initiation and Figure 7 shows module after crack initiation and propagation in solder layer for thermal cycle -55°C to 160°C .

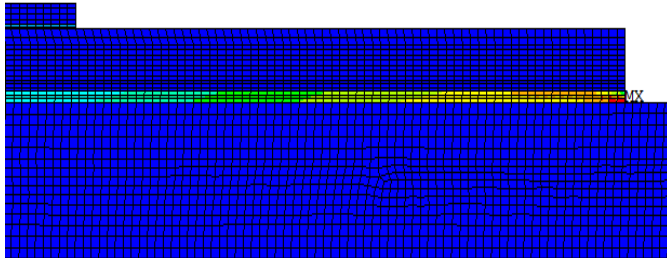


Figure 6: 2D IGBT module before crack initiation.

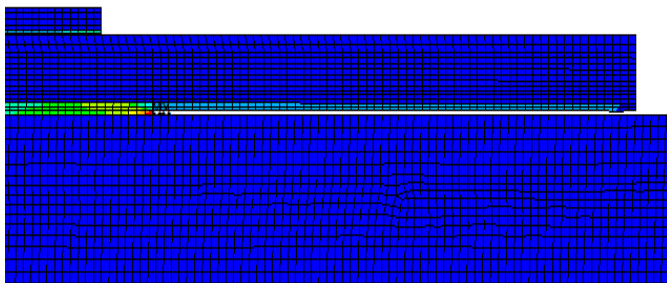


Figure 7: 2D IGBT module after crack initiation and propagation.

V. CONCLUSION

In this paper, 2D finite element analysis of a multilayered IGBT module under thermal cyclic loading is carried out. Damage is calculated in individual elements using E-P model coupled with SI technique. Using threshold damage criteria, the elements are killed. The crack is initiated at the outer side of the bottom solder layer interface in between base plate and substrate due to CTE mismatch. The crack is propagated towards the inner side of the bottom solder layer till it is completely delaminated. As a result delamination of solder layer, IGBT module fails to carry any further mechanical and electrical loads. Parametric study performed for IGBT module. Considered thermal cycles -55°C to 160°C and 0°C to 100°C , we get number of cycles to failure are 2266 and 2600 respectively. Thus fatigue life is predicted for solder interconnects in IGBT module. Conclusion of above parametric study is thermal cycle ΔT value decreases the number of cycles to failure increases. Future work will involve fatigue life prediction of the IGBT module by comparing various solder alloys with different thermal cycles.

REFERENCE

[1] Mika Ikonen, "Power Cycling Lifetime Estimation of IGBT Power Modules Based on Chip Temperature

Modeling", Lappeenranta University of Technology, Lappeenranta, Finland, pp 21, 11th of December, 2012.

[2] IGBT Application Handbook, HBD87/D, Rev 2 Sep-2012.

[3] Leila JannesariLadani, "Damage Initiation and Evolution in Voided and Unvoided Lead Free Solder Joints Under Cyclic Thermo-Mechanical Loading", PhD dissertation, University of Maryland, College Park, 2006.

[4] James D. Gyllenskog, "Fatigue Life Analysis of T-38 Aileron Lever Using a Continuum Damage Approach", PhD dissertation, Utah State University, Logan, Utah, 2010.

[5] Hua Ye, Minghui Lin, CemalBasaran, "Failure Modes and FEM Analysis of Power Electronic Packaging", UB Electronic Packaging Laboratory, State University of New York at Bu_alo, 101 Ketter Hall, North Campus, Bu_alo, NY 14260-4300, USA.

[6] Z. Sun, L. Benabou, P.R. Dahoo, "Prediction of thermo mechanical fatigue for solder joints in power electronics modules under passive temperature cycling", Engineering Fracture Mechanics 107 (2013) 48–60.

[7] N.Y.A. Shammas, M.P. Rodriguez, A.T. Plumpton and D. Newcombe, "Finite Element Modelling of Thermal Fatigue Effects in IGBT Modules", IEE Proc. Circuits Devices Syst. Vol. 14X, No. 2. April 2001.

[8] GayatriCuddalorepatta, "Evolution of the Microstructure and Viscoplastic Behavior of Microscale SAC305 Solder Joints as a Function of Mechanical Fatigue Damage", PhD dissertation, University of Maryland, College Park, 2010.

[9] Leila JannesariLadani, "Damage Initiation and Propagation in Voided Joints", Department of Mechanical and Aerospace Engineering, Utah State University, Logan, UT, 84341.

[10] Daniel M Farley, Professor AbhijitDasgupta, "Development of Fatigue Models for Copper Traces on Printed Wiring Assemblies Under Quasi-static Cyclic Mechanical Bending", PhD dissertation, University of Maryland, College Park, 2010.